Energy 286 (2024) 129583

Contents lists available at ScienceDirect

Energy

journal homepage: www.elsevier.com/locate/energy

Hybrid particle swarm and sea horse optimization algorithm-based optimal reactive power dispatch of power systems comprising electric vehicles

Hany M. Hasanien [a,b,*], Ibrahim Alsaleh [c], Marcos Tostado-Véliz [d], Miao Zhang [e], Ayoob Alateeq [c], Francisco Jurado [d], Abdullah Alassaf [c]

[a] Electrical Power and Machines Department, Faculty of Engineering, Ain Shams University, Cairo, 11517, Egypt
[b] Faculty of Engineering and Technology, Future University in Egypt, Cairo, 11835, Egypt
[c] Department of Electrical Engineering, College of Engineering, University of Hail, Hail, 55211, Saudi Arabia
[d] Department of Electrical Engineering, University of Jaén, 23700, Linares, Spain
[e] Beijing Sifang Automation Co., Ltd, Beijing, 100080, China

ARTICLE INFO

Handling Editor: Prof X Ou

Keywords:
Electric vehicles
Optimal reactive power dispatch
Sea horse optimization

ABSTRACT

The reliability and effectiveness of today's electrical grids rely heavily on optimal reactive power dispatch (ORPD). The ORPD problem gets more challenging to resolve in the setting of ever-increasingly dynamic and complex systems. To handle the ORPD while also considering the existence of electric vehicles, this research introduces a novel technique: the Hybrid Particle Swarm Optimization and Sea Horse Optimization (PSOSHO) algorithm. Byreducing both active power loss and voltage variation, the proposed PSOSHO approach aims at improving the efficiency and reliability of the power grid. Simulation studies on reference power grids, including the IEEE 30-bus and IEEE 57-bus networks, verified its efficacy. Existing metaheuristic optimization techniques are compared using the same restrictions, governing parameters, and data. The results show that the PSOSHO method is trustworthy and effective in resolving the ORPD problem. One of the most pressing issues facing today's electricity grids is how to accommodate the growing number of electric vehicles. Real data on electric vehicles are incorporated in the analyses to obtain a realistic study. The suggested PSOSHO algorithm is a significant step forward in this area, providing a reliable and effective answer to the problem of optimum reactive power dispatch and helping to ensure the long-term viability of power systems in the age of electromobility.

1. Introduction

For electric networks with a large concentration of electric vehicles (EVs), optimal reactive power dispatch (ORPD) remains of utmost importance [1,2]. Since more and more EVs and other dynamic demands are incorporated into the electric grid [3,4], the difficulty of controlling reactive power rises to new heights [5]. The ORPD problem represents the complex swap between lowering actual power losses and keeping system voltage within allowable limits [6]. It is characterized by its non-linearity, non-convexity, and multi-objective nature. Its ideal solution is crucial for fitting EVs' charging and discharging patterns [7], minimizing power losses, and improving voltage stability. By analyzing the system's real power losses and voltage deviation (VD), ORPD calculates the best values for generator voltages, transformer tap settings, and reactive power compensators to achieve the desired results.

EVs can potentially significantly affect the ORPD problem because of their distinct features, such as their varied charging/discharging cycles and capacity to offer reactive power input [8]. For instance, EVs are charged during off-peak hours and released during peak times [9]. In addition to supporting the grid's voltage profile, EVs may offer reactive power assistance. For power systems with extensive integration of EVs, ORPD is crucial since it may assist in improving the following problems: 1) Real power losses may rise because of the added demand that EVs create on the power system [10]. ORPD is an optimization problem that helps reduce real power losses; 2) Voltage stability issues, as EVs might stress the power network at high charging times [11]. ORPD may improve system voltage by improving reactive power flow and guaranteeing enough reactive power compensation [12]. Overall, ORPD is an indispensable instrument for studying and operating power networks, particularly those with a significant penetration of EVs [13]. ORPD can aid in mitigating the difficulties faced by EVs and ensure the electric grid's safe and dependable functioning [14].

* Corresponding author. Electrical Power and Machines Department, Faculty of Engineering, Ain Shams University, Cairo, 11517, Egypt.
E-mail address: hanyhasanien@ieee.org (H.M. Hasanien).

https://doi.org/10.1016/j.energy.2023.129583
Received 22 October 2023; Received in revised form 1 November 2023; Accepted 3 November 2023
Available online 3 November 2023

The master goals of the ORPD problem are to reduce active power losses [15] as well as maintain voltage profiles at load buses within predetermined tolerances to ensure the stability and power quality of the network [16]. This is done by optimizing the allocation of reactive power resources within a power grid. In addition to these primary goals, ORPD may be utilized to accomplish secondary goals, including emissions reduction, power quality improvement, and reliability improvement [17]. Due to its non-linear, non-convex character, addressing the ORPD problem has historically proved challenging [18]. Traditional optimization approaches like linear programming [19,20], as well as quadratic programming [21] suffer from their limits when tackling these complex goals. The best solution for large and complicated power grids is not always found using traditional approaches since they may be computationally costly. Furthermore, traditional methods could be susceptible to the original initial position and may stuck in a local optimal solution [22]. Therefore, these traditional approaches often find it challenging to handle the dynamic and time-varying demands, such as the variable EV charging/discharging cycles that are becoming more common in contemporary power networks [23]. Heuristic optimization methods have become adequate resources for resolving the ORPD optimization problem in response to these difficulties [24]. The ORPD problem may often be solved using heuristic methods in a reasonable timeframe [25]. Such heuristics, which incorporate GA, evolutionary algorithms, as well as PSO, provide a more adaptive and flexible method of traversing the intricate ORPD optimum solution. The PSO algorithm has grown in popularity because of its effectiveness in exploring and taking advantage of the solution space, making it a good choice for handling the complexities of ORPD in the presence of EVs.

An innovative metaheuristic optimization method, the sea horse optimization algorithm (SHO), has been developed in response to observations of seahorses' mobility, hunting, and breeding behavior. The SHO algorithm was first proposed in 2022 by Zhao et al. [26]. By sustaining a population of seahorse-like individuals, the SHO algorithm functions. Every individual is a possible response to the optimization problem. The location of each member of the population is then repeatedly updated by the SHO method following the natural mobility, hunting, and reproduction patterns of seahorses [27]. The Levy flying mechanism served as the model for seahorse movement behavior, favoring giant leaps over deliberate movements. The capacity of seahorses to alter their color and meld into their environment gives rise to their distinctive hunting behavior. Seahorses' monogamous lifestyle and distinctive courting ritual are the main influences on how they reproduce. The breeding behavior is described via a crossover and mutation process in the SHO algorithm. It has been shown that the SHO method efficiently resolves several optimization problems, including benchmark functions and engineering problems.

The hybridization process entails merging two or more optimization techniques to produce a new hybrid approach that combines the best features of the original methods [28,29]. Optimization technique performance may be enhanced by hybridization regarding solution quality and convergence speed [30]. In this context, this research offers the PSOSHO algorithm, a unique heuristic technique that combines the benefits of PSO and SHO to address the problems with ORPD in EV-integrated power systems. This novel strategy intends to improve the robustness and effectiveness of contemporary power systems, guaranteeing their smooth adaptation to the developing electric transportation environment. To achieve the best design variables for the best result for the ORPD problem, Including and excluding the use of EVs, the PSOSHO method is proposed in the research. The IEEE 30-, and 57-bus networks, two benchmark electric power networks, are used to implement the ORPD. The goals of this study are (i) minimizing real power loss and (ii) minimizing voltage variation of the PQ buses. The relevant publications show and contrast the simulation results for each aim with the most recently published optimization approaches. Using actual EV data and load profiles, the two goals are performed with the inclusion of EVs. The PSOSHO proposal's usefulness and efficacy as an optimization method for implementing ORPD are established. Explicitly, this paper's contribution may be summed up as follows:

- A hybrid PSOSHO algorithm is produced as a novel metaheuristic optimization algorithm.
- The proposed hybrid algorithm is efficiently used to solve the ORPD problem.
- EV charging locations are inserted into the studied power grids.

This article's remaining sections are structured as follows: The mathematical expression of the investigated goals is presented in the second part. An overview of the PSOSHO is provided in the third section. The simulation findings are offered in the fourth section. The article's summary is included in the fifth one.

2. Problem Formulation

The objective function in the ORPD optimization problem is a non-linear function whose solution requires satisfying both minimum and maximum limits [31]. Here is a mathematical illustration of the objective:

$$\text{Min } F(x,u) \tag{1}$$

$$\text{Subject to: } g(x,u)=0,\ h(x,u)\leq 0 \tag{2}$$

The target of the ORPD problem is finding the values of three design parameters, the PV bus voltage, the tap settings of the transformer, and the VAR injected, that provide the best possible system performance. All of these design factors may be summed up as:

$$u^T=\left[V_{G_1}\ldots V_{G_{NGen}},Q_{C_1}\ldots Q_{C_{NCom}},T_1\ldots T_{NTr}\right] \tag{3}$$

In addition, the dependent variables can be written as:

$$x^T=\left[V_{L_1}\ldots V_{L_{NLB}},Q_{G_1}\ldots Q_{G_{NGen}},S_{l_1}\ldots S_{l_{Nline}}\right] \tag{4}$$

The target of the ORPD optimization problem is to reduce the effects of actual power losses as well as voltage swings. Mathematically, the ORPD problem is stated in Ref. [22].

2.1. The fitness functions

Reducing actual power losses and limiting voltage fluctuations at the PQ buses are both goals of the ORPD optimization problem. Minimizing power loss is shown by equation (5) [12].

$$\min F_1=P_L=\sum_{k\in N_l}P_k^{loss}=\sum_{k\in N_l}G_k\left(V_i^2+V_j^2\text{-}2V_iV_j\cos\theta_k\right) \tag{5}$$

where, V_i and V_j define the voltages at i and j. G_k denotes the conductance of the branch linking bus i with bus j. Furthermore, minimizing VD at the PQ buses is described by equation (6):

$$\min F_2=VD=\sum_{i=1}^{N_{Load}}\left|V_i\text{-}V_{ref}\right| \tag{6}$$

where, N_{Load} is the number of load buses.

2.2. Power network constraints

2.2.1. Equality constraints formulation

The following mathematical expressions are the equality restrictions [12]:

$$P_{gi}\text{-}P_{di}\text{-}V_i\sum_{j=1}^{N_B}V_j(G_k\cos\theta_k+B_k\sin\theta_k)=0 \tag{7}$$

$$Q_{gi}+Q_{ci}\text{-}Q_{di}\text{-}V_i\sum_{j=1}^{N_B}V_j(G_k\sin\theta_k\text{-}B_k\cos\theta_k)=0,\ i\ \epsilon N_{Load} \tag{8}$$

where B_k refers to the susceptance of the branch linking buses i and j. P_{gi} as well as Q_{gi} define the produced power. P_{di} and Q_{di} are the demand real and reactive power, respectively. Q_{ci} is the compensator reactive power.

2.2.2. Inequality constraints formulation

These restrictions may be stated quantitatively by the following equations [12]:

$$V_i^{min} \le V_i \le V_i^{max}, i\epsilon N_B \tag{9}$$

$$T_m^{min} \le T_m \le T_m^{max}, m\epsilon N_t \tag{10}$$

$$Q_{gi}^{min} \le Q_{gi} \le Q_{gi}^{max}, i\epsilon N_{pv} \tag{11}$$

$$Q_{ci}^{min} \le Q_{ci} \le Q_{ci}^{max}, i\epsilon N_c \tag{12}$$

$$P_s^{min} \le P_s \le P_s^{max} \tag{13}$$

$$S_k \le S_k^{max}, k\epsilon N_l \tag{14}$$

where T_m defines the variation in transformer tapping, N_{pv} is the PV busses. N_t is the transformer tapings. P_s is the active power at the swing bus, of limits P_s^{min} as well as P_s^{max}. S_l defines the power of branch l.

3. The introduced PSOSHO technique

3.1. The seahorse optimizer

The Seahorse Optimizer (SHO) was recently published as it was first introduced by Zhao et al., in 2022 [26]. The SHO is an innovative swarm intelligence-based metaheuristic algorithm that takes cues from the natural behavior of seahorses regarding foraging, predatory interactions, and reproduction. By emulating seahorses' varied movement patterns and probabilistic predation mechanisms, SHO balances local exploitation and broad exploration. In addition, SHO helps boost population variety since it breeds children while preserving the beneficial information of the male parent.

It is essential to strike a balance between these two goals. Therefore, the mobility and predation behaviors are tailored to use search tactics. After completing these two actions, the breeding activity is carried out. This section will go into further detail in expressing and discussing the mathematical models of these parts.

The SHO algorithm starts with the initiation of the population. It can be expressed as [26]:

$$Seahorses = \begin{bmatrix} x_1^1 & \cdots & x_1^{Dim} \\ \vdots & \ddots & \vdots \\ x_{pop1}^1 & \cdots & x_{pop}^{Dim} \end{bmatrix} \tag{15}$$

X_{elite} represents the best-fit candidate whose equation:

$$X_{elite} = argmin(f(X_i)) \tag{16}$$

where $f(X_i)$ is the fitness function.

3.1.1. The movement behavior of sea horses

The sea horses' behaviors are pretty close to the normal distribution. The actions may be broken down into two categories: exploration and exploitation. In the first, the sea horse swims in a circular pattern, creating a vortex in the water. The exploitation is evident in it. The sea horses are heading towards the X_{elite}'s direction. The Levy flight [32] is used to model the distance traveled. This situation has a mathematical expression that goes like this:

$$X_{new}^1(t+1) = X_i(t) + Levy(\lambda)(X_{elite}(t) - X_i(t)) \times x \times y \times z + X_{elite}(t)) \tag{17}$$

where x, y, and z are the three-dimensional components. They help update the positions of candidate solutions. The Levy function is calculated as follows [33]:

$$Levy(z) = s \times \frac{w \times \sigma}{|k|^{\frac{1}{\lambda}}} \tag{18}$$

where λ is a random number chosen from [0, 2]. s equals 0.01. w and k are randomly selected from [0, 1]. σ is computed as follows:

$$\sigma = \left(\frac{\Gamma(1+\lambda) \times sin\left(\frac{\pi\lambda}{2}\right)}{\Gamma\left(\frac{1+\lambda}{2}\right) \times \lambda \times 2^{\left(\frac{\lambda-1}{2}\right)}} \right) \tag{19}$$

Brownian motion [34] with sea waves is the second motion considered here. The sea horse's mobility is so that it may more effectively explore the search space. In this context, its mathematical expression is as follows:

$$X_{new}^1(t+1) = X_i(t) + rand \times l \times \beta_t \times (X_i(t) - \beta_t \times X_{elite}) \tag{20}$$

where l is a constant coefficient. β_t is the random walk coefficient, which is calculated as follows:

$$\beta_t = \frac{1}{\sqrt{2\pi}} \times e^{\left(\frac{-x^2}{2}\right)} \tag{21}$$

3.1.2. The predation behavior of sea horses

Assuming a 90 % chance of success, a random number of 0 or 1 is created to differentiate between the sea horse's success and failure in capturing food. The success of the predation highlights the exploitation since the elite represents the status of the victim. If the predation is successful, the sea horse will outrun its target and successfully catch it. In contrast, when the predation attempt fails, the reaction time is the inverse, suggesting the patterns to explore. Here is the corresponding mathematical expression:

$$X_{new}^2(t+1) = \begin{cases} \alpha \times \left(X_{elite} - rand \times X_{new}^1(t)\right) + (1-\alpha) \times X_{elite} if r_2 > 0.1 \\ (1-\alpha) \times \left(X_{new}^1(t) - rand \times X_{elite}\right) + \alpha \times X_{new}^1(t) if r_2 \le 0.1 \end{cases} \tag{22}$$

where X_{new}^1 is the updated position. r_2 is the random number ranging from 0 to 1. α is calculated as follows:

$$\alpha = \left(1 - \frac{t}{T}\right)^{\frac{2t}{T}} \tag{23}$$

where T is the maximum number of iterations. The method may be made to converge to a solution by adjusting the value of the parameter α.

3.1.3. The reproduction performance of sea horses

According to fitness, the search agents are divided in half. The algorithm picks half of the people as dads and the other half as mothers to inherit desirable qualities for the next generation. This phase is mathematically represented as follows:

$$X_i^{offspring} = r_3 X_i^{father} + (1 - r_3)^{X_i^{mother}} \tag{24}$$

where r_3 is a number chosen randomly between 0 and 1.

3.2. The hybrid PSOSHO

In this study, a novel hybridization between PSO and SHO. The hybridization of PSO and SHO may use the benefits of both algorithms to develop a new method that is even more successful in handling ORPD problems. For example, this hybrid algorithm may use the efficiency and resilience of PSO and the ability to strike a balance between the exploration and exploitation offered by SHO. In the PSO algorithm, These candidates have positions and velocities, updated mathematically in Eqs. (25) and (26) [35]:

$$X_{ij}^{t+1} = X_{ij}^{t} + v_{ij}^{t+1} \tag{25}$$

$$v_{ij}^{t+1} = wv_{ij}^{t} + C_1\left(X_{ij}^{p(t)} - X_{ij}^{t}\right) + C_2\left(X_{j}^{g(t)} - X_{ij}^{t}\right) \tag{26}$$

where X_{ij}^{t} and v_{ij}^{t} define the location as well as the velocity of the agent. w is the inertia weight. C is the acceleration coefficient. Furthermore, the flowchart of the hybrid PSOSHO is presented in Fig. 1.

4. Interpretation of the simulation results

The results of implementing and testing the suggested approach for ORPD on IEEE 30-, and 57-bus networks are explored in depth in the current section of the paper. Using data from the IEEE, the 30-bus power system has 3 shunt compensators, 21 loads, 41 transmission lines, and 5 PV buses [36]. With the IEEE standard 57-bus system, the reference power grid has 80 transmission lines, 3 shunt capacitors, and 6 PV buses. To learn more about both systems, we optimize for two criteria. The demonstration of these couple goals is presented in a couple of parts: one discusses the real Power losses reduction, case 1, and the other one, case 2, discusses the results in which the VD of the load buses is reduced. Mathematically, the objective functions are rewritten by including

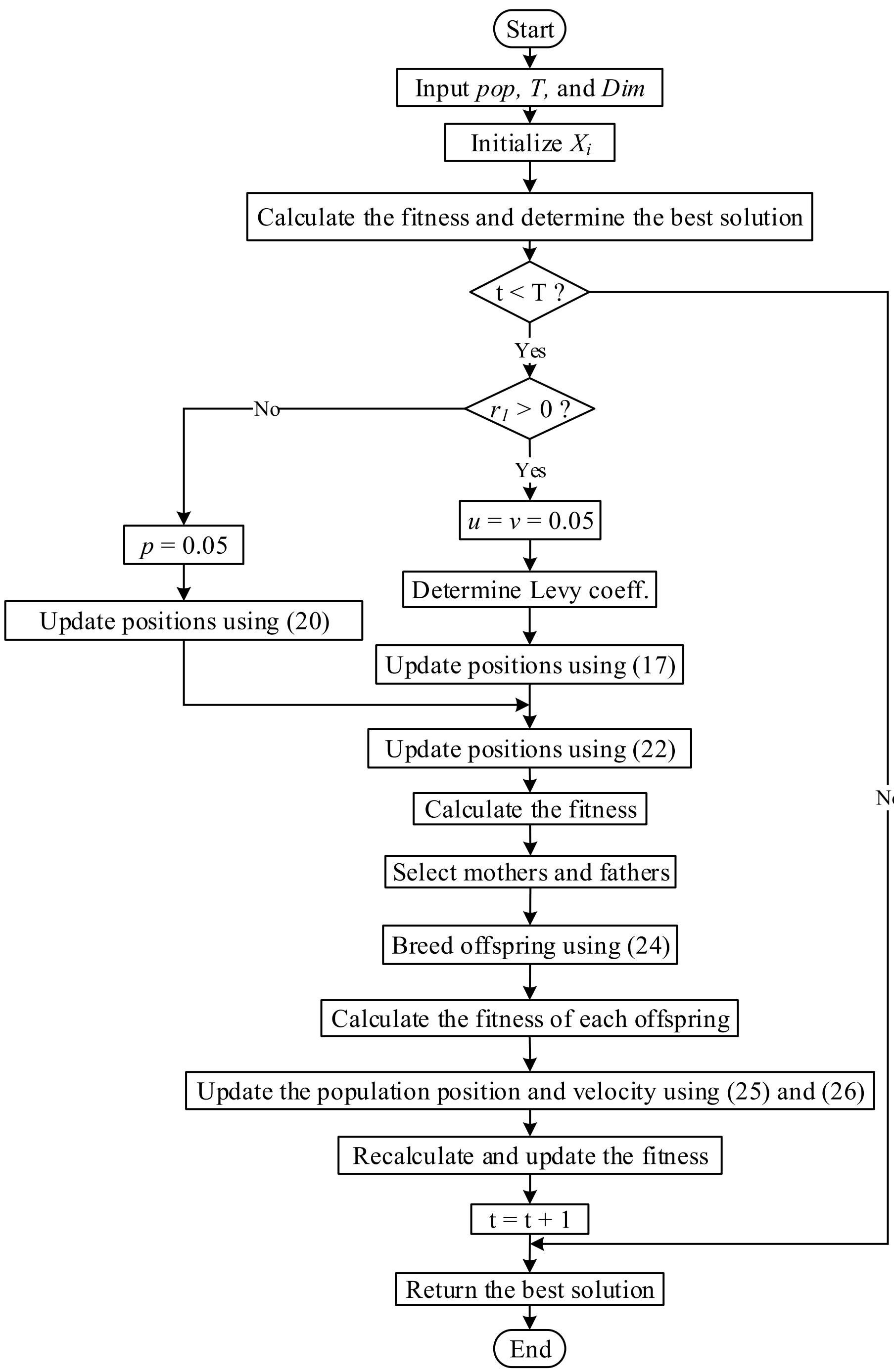

Fig. 1. Flowchart of the proposed hybrid PSOSHO.

significant penalty factors to filter out solutions beyond the constraints. To solve the ORPD problem, MATLAB is used as the development platform. When solving ORPD optimization problems, the matpower toolbox is pre-loaded with m-files containing data from the investigated benchmark power systems. This research used the Lenovo IdeaPad 330 ″Up to 8th Gen Intel® Quad Core i7-8550U" to run the system simulations and ORPD. In all of the situations that are examined, 600 iterations are performed.

4.1. Power loss minimization results

4.1.1. The IEEE 30-bus network

The IEEE 30-bus benchmark network takes into account 19 predetermined control variables, including voltage magnitudes on buses 1, 2, 5, 8, 11, and 13; tap settings on transformers; and the amount of reactive power inserted into buses 10, 12, 15, 17, 20, 21, 23, 24, and 29. Voltage levels may vary between 1.06 and 0.94 p.u., respectively. The transformer's taps should be in the range of 1.1 to 0.9. Shunt capacitor reactive power ranges from zero to twenty, seven, ten, six, ten, and six MVARs.

The simulation results for minimizing power loss using the proposed PSOSHO are shown in Table 1, together with those obtained using various meta-heuristic methods (GA, PSO, firfly algorithm (FA), artificial bee colony (ABC), and bacteria foraging optimization algorithm (BFOA)). The PSOSHO's optimum search agents that generated these optimal results are listed in Table 2. Fig. 2 shows how the PSOSHO, PSO, and MPA algorithms converge to the optimal solution of the power loss reduction problem within 600 iterations. The findings of the various optimization methods show rapid convergence. The PSOSHO performed marginally better than the competing methods.

4.1.2. The IEEE 57-bus network

There are 27 control parameters in play here, including the voltage levels on buses 1, 2, 3, 6, 8, 9, and 12; the tap settings of 15 transformers; and the VAR compensators on buses 18, 25, and 53. All design variables' voltage magnitudes must fall between 1.06 and 0.94 p.u. The tap positions on the transformer should be between 1.1 and 0.9. A value between −20 and 20 MVARs is required for the VAR adjustment. The minimal power losses attained by the PSOSHO, ETSO, MPA, and PSO are listed in Table 3. Meanwhile, Table 4 provides the optimal design parameters of the 57-bus network for the first objective. Fig. 3 plots a comparison between the convergence performance of the first objective for the PSOSHO, MPA, PSO, and ETSO algorithms over 600 iterations. It can be noticed that the PSO converges after the other algorithms by many iterations, whereas the proposed PSOSHO method converges fast and first.

4.2. Voltage deviation minimization results

In the second scenario, reducing VD at load buses is the primary focus. The following two parts provide the specific case outcomes for the examined benchmark test systems.

4.2.1. The IEEE 30-bus network

The 30-bus network's VD minimization at the PQ buses is carried out using the suggested PSOSHO, and the results are compared with those of other optimization methods. Table 5 presents the contrast. Additionally, Table 6 lists the best design parameters determined by the proposed PSOSHO. Fig. 4 depicts the convergence behavior of the second objective, which PSOSHO, in addition to PSO, GA, and PSOGWO, acquired after 600 iterations. It can be observed that the suggested PSOSHO converges quickly and only requires less than 100 iterations to get the best comparative result.

4.2.2. The IEEE 57-bus network

The values of the simulation results are listed in Table 7 for the second goal from the proposed PSOSHO compared with the results obtained from other optimization techniques for the same objective described in the literature. Additionally, Table 8 displays the ideal design parameters that match the PSOSHO's ideal solution. Fig. 5 presents the convergence characteristics of the PSOSHO, ETSO, PSO, and MPA algorithms when applied to the VD minimization optimization problem, as measured by their convergence curves after 600 iterations. It can be seen that the PSOSHO method needs less than 100 iterations to get a better solution than the other optimization methods.

Table 2
Design variables of the 30-bus system optimized for power loss minimization.

Design variables	**|V| at bus 1**	**1.03084719**
	2	1.021064384
	5	1.023562353
	8	1.047179507
	11	0.982424285
	13	1.011043263
	'Q' compensation at bus 10	0.262960736
	12	0
	15	2.193818718
	17	1.947835398
	20	1.766263523
	21	4.481739259
	23	1.219706308
	24	1.620051841
	29	1.192551495
	Transformer setting at branch11	0.975658468
	12	1.043358393
	15	0.968128787
	36	0.94520611

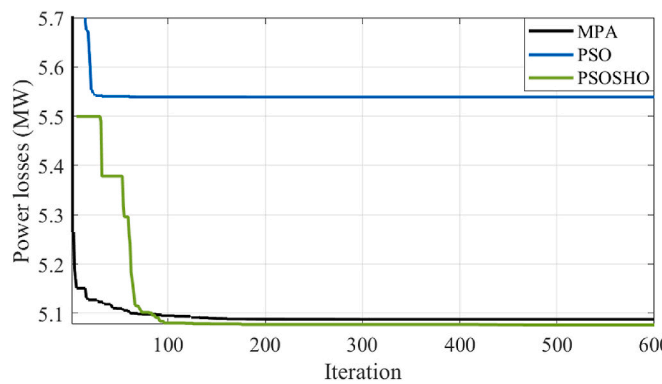

Fig. 2. Convergence curves of the first objective for the 30-bus network.

Table 3
Objective Values for Power Loss Minimization in the 57-bus system.

Algorithm	PSOSHO	ETSO [12]	MPA [12]	PSO [12]
Power Losses (MW)	25.47153743	25.4963	26.89276024	29.535

Table 1
Objective Values for Power Loss Minimization in the 30-bus system.

Algorithm	PSOSHO	ETSO [12]	PSOGWO [22]	GA [22]	PSO [22]	FA [22]	ABC [22]	BFOA [22]
P_{loss} (MW)	5.0763872	5.0766	5.0903652	5.0977	5.1041	5.64	5.79	10.01

Table 4
Design variables of the 57-bus system optimized for power loss minimization.

Design variables	**1**	**1.042476727**
	2	1.007393742
	3	0.956587887
	6	0.992498592
	8	0.964910714
	9	0.941827787
	12	0.953957102
	Reactive power compensation at bus 18	−1.887694004
	25	8.507735231
	53	20
	Transformer setting at branch19	0.900007787
	20	1.013729424
	31	1.023128753
	35	1.062653368
	36	0.964561455
	37	1.006490025
	41	0.957583845
	46	0.941244149
	54	0.933449741
	58	0.961657671
	59	0.955341112
	65	0.943944621
	66	0.92540014
	71	0.934128663
	73	1.005119814
	76	1.005395429
	80	0.94613289

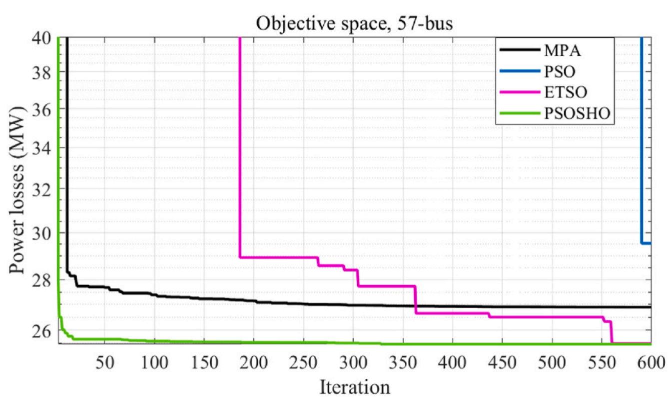

Fig. 3. Convergence curves of the first objective for the 57-bus network.

Table 5
Objective Values for VD Minimization in the 30-bus system.

Algorithm	PSOSHO	PSOGWO [22]	PSO [22]	GA [22]	GSA [22]
VD (p.u)	0.26719409	0.278	0.2816	0.3732	0.4672

4.3. Electric vehicles integration in ORPD

The implications of adding EV charging stations to power systems have been well examined. To make room for EVs, the suggested optimization problem is enlarged. The ORPD optimization problem is solved using the PSOSHO algorithm in power networks with EV charging stations. An expanded ORPD analysis is carried out in the context of the 30- and 57-bus networks to include EV charging stations, hence adding a dynamic load situation. The demand profiles of plug-in e-cars are used in place of the typical system loads, reflecting EVs' actual energy consumption patterns. A total of 1000 plug-in e-cars are placed at two particular buses in the power system, notably buses 15 and 16, to mimic this situation. These charging stations are simulated for data from Miami, Florida, and Bowling Green, Kentucky, in the United States, and they make use of data curves that depict regional charging patterns [37].

Table 6
Design variables of the 30-bus system optimized for VD minimization.

Design variables	**|V| at bus 1**	**1.06**
	2	0.94
	5	0.94
	8	0.94
	11	1.06
	13	0.94
	'Q' compensation at bus 10	0
	12	0
	15	0
	17	0
	20	0
	21	0
	23	2.736902276
	24	0
	29	0
	Transformer setting at branch 11	0.999461588
	12	1.1
	15	1.1
	36	0.962562403

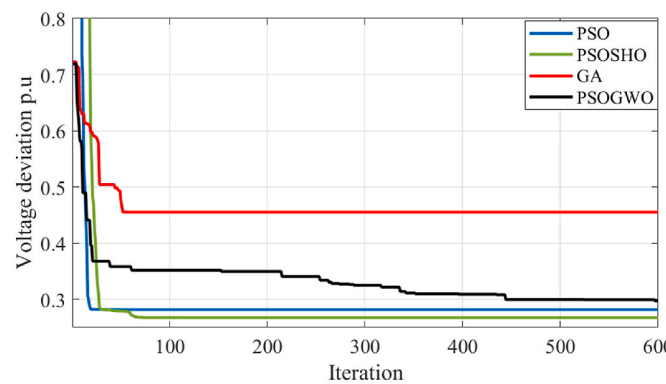

Fig. 4. Convergence curves of the second objective for the 30-bus network.

Table 7
Objective Values for VD Minimization in the 57-bus system.

Algorithm	PSOSHO	MPA [12]	ETSO [12]	PSO [12]
VD (p.u)	0.68288123	0.685217269	0.799021	0.9066

With an average daily trip distance of 25 miles in addition to an ambient temperature of 20 °C, each station represents the features of EVs existing in different localities. In addition, sedans are expected to make up 80 % of the plug-in cars in these fleets. Fig. 6 shows the resultant EV demand shapes for Bowling Green and Miami, demonstrating how the daily variation in power consumption may be seen [38].

The results of the hourly first objective for the 30-bus network are shown in Fig. 7. The minimum value of the first objective is at its peak at 1 a.m. in Bowling Green, Kentucky, and at 3 a.m. in Miami, Florida.

Likewise, The VD minimization solutions for the 30-bus system, on an hourly basis, are shown in Fig. 8. The minimum values of the second objective can be noted to happen between 10 and 11 a.m. in the two studied locations.

Similarly, The outcomes of the hourly first objective for the 57-bus network are shown in Fig. 9. The minimum value of the first objective is at midnight in Bowling Green, Kentucky, and at 5 a.m. in Miami, Florida.

Furthermore, in the second objective, the hourly results for the 57-bus network are shown in Fig. 10. The minimum values of the second objective can be noted to happen at 2 a.m. in Bowling Green, Kentucky, and at 4 p.m. in Miami, Florida.

Table 8
Design variables of the 57-bus system optimized for VD minimization.

Design variables	1	1.018546404
	2	1.027836846
	3	1.003085093
	6	0.959037498
	8	0.94280794
	9	0.973577718
	12	1.021419462
	Reactive power compensation at bus 18	−1.429628833
	25	2.229883182
	53	17.07762748
	Transformer setting at branch19	0.997330706
	20	0.963172125
	31	0.98278313
	35	1.075184895
	36	0.9
	37	1.01603678
	41	0.964573926
	46	0.919173972
	54	0.9
	58	0.970433695
	59	0.975291423
	65	0.988196592
	66	0.9
	71	0.937264857
	73	1.029569225
	76	0.9
	80	0.974250207

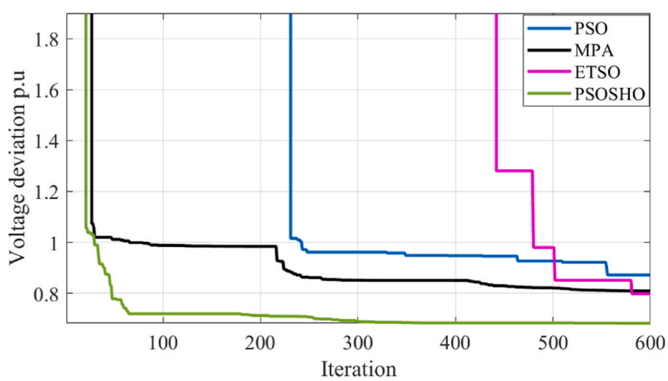

Fig. 5. Convergence curves of the second objective for the 57-bus network.

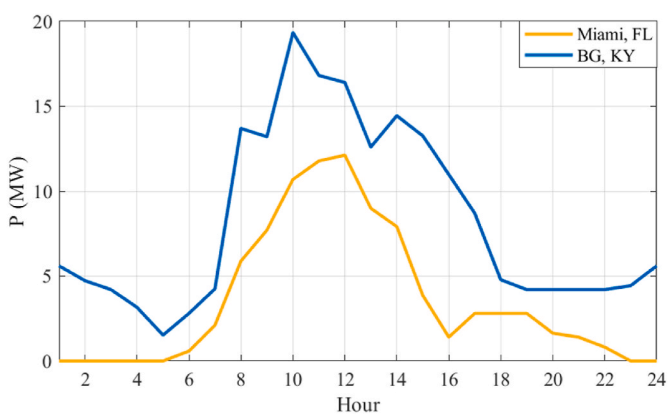

Fig. 6. Weekday electric load profile per plug.

5. Conclusions

To get the best ORPD solution in electrical power networks integrating EVs, this research introduced a new optimization technique called PSOSHO. The suggested study methodology successfully reduces power losses and VD. On two standard electric networks, namely the IEEE 30, as well as 57 bus networks, the suggested PSOSHO approach is put to the test. The ORPD problem is addressed in the thorough analysis by PSOSHO while reducing actual power losses and voltage variation. The multifaceted impacts of EV presence on the two objectives are also explored. By contrasting the suggested PSOSHO with several heuristic strategies described in recent literature, the proposed PSOSHO is assessed. The PSOSHO demonstrated its capacity to provide superior solutions for the investigated optimization problem from the acquired findings and comparative graphic. We concluded that using the PSOSHO

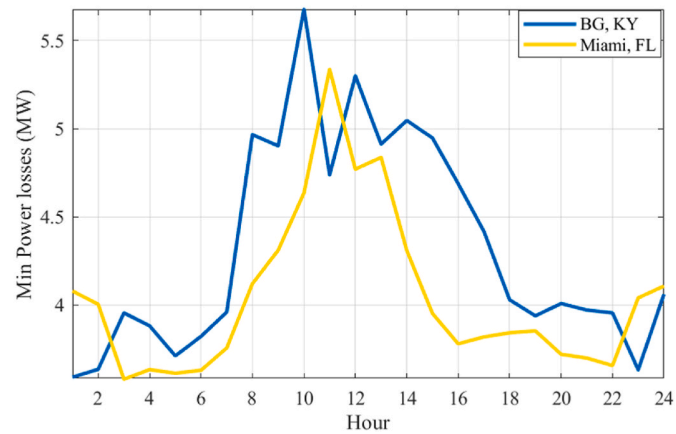

Fig. 7. Hourly Variation in P_{Loss} of the 30-bus network.

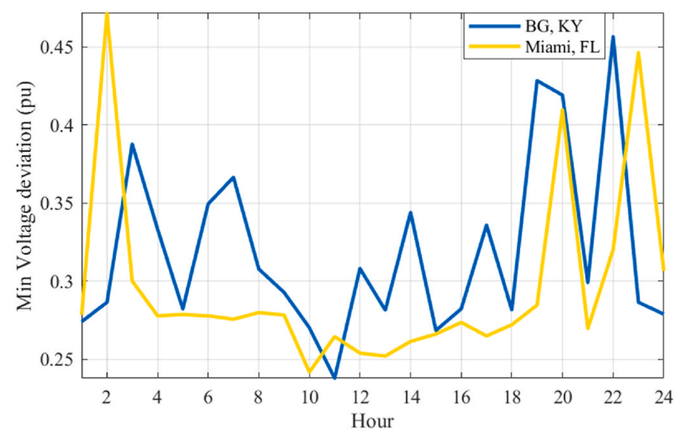

Fig. 8. Hourly Variation in VD of the 30-bus system.

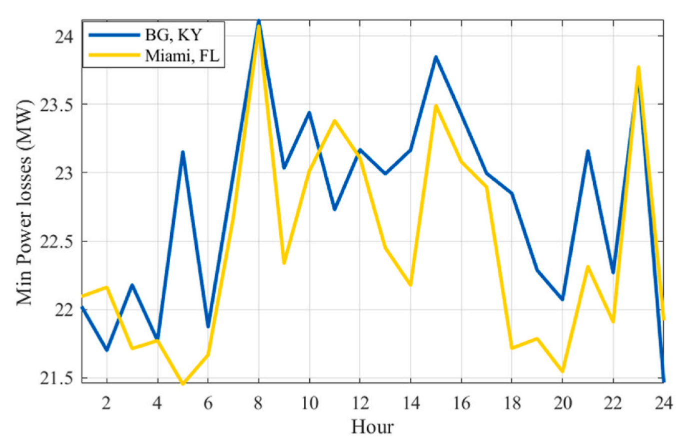

Fig. 9. Hourly Variation in P_{Loss} of the 57-bus network.

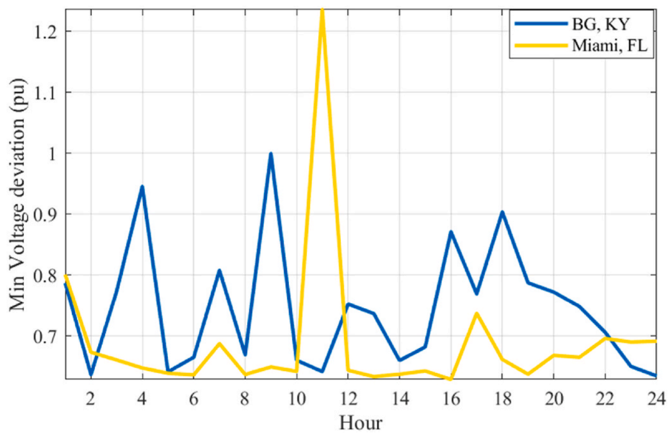

Fig. 10. Hourly Variation in VD of the 57-bus system.

approach improved the first goal by 0.006 % 0.27 %, 0.4 %, 0.5 %, 11 %, 14 %, and 49 % compared to ETSO, PSOGWO, GA, PSO, FA, ABC, and BFOA, respectively, in the 30-bus system. Moreover, the simulation findings demonstrate an improvement in the second target of minimizing voltage variation by 4 %, 5 %, 34 %, and 42 % compared to PSOGWO, PSO, GA, and GSA, respectively, in the 30-bus network. Finally, the total outcomes show that the PSOSHO algorithm offers more optimum solutions for the ORPD problem than the other reported methodologies. The proposed PSOSHO is recommended for solving more optimization problems in power systems.

Credit author statement

Hany M. Hasanien: Conceptualization, Methodology, Formal analysis, Writing – original draft, Ibrahim Alsaleh, Marcos Tostado-Véliz, Miao Zhang, Abdullah Alassaf, Ayoob Alateeq and Francisco Jurado: Editing, Validation, Investigation.

Declaration of competing interest

The authors declare that they have no known competing financial interests or personal relationships that could have appeared to influence the work reported in this paper.

Data availability

Data will be made available on request.

Acknowledgement

This research has been funded by Scientific Research Deanship at University of Ha'il - Saudi Arabia through project number <<RG-23 171>>.

References

[1] Pg AK, P AJ, D D. Hybrid CAC-DE in optimal reactive power dispatch (ORPD) for renewable energy cost reduction. Sustain Comput: Info Syst 2022;35. https://doi.org/10.1016/j.suscom.2022.100688.
[2] Jiang T, Dong X, Zhang R, Li X. Strategic active and reactive power scheduling of integrated community energy systems in day-ahead distribution electricity market. Appl Energy 2023;336. https://doi.org/10.1016/j.apenergy.2022.120558.
[3] Ali A, et al. A Bi-level techno-economic optimal reactive power dispatch considering wind and solar power integration. IEEE Access 2023;11:62799–819. https://doi.org/10.1109/ACCESS.2023.3286930.
[4] Tang M, Zhuang W, Li B, Liu H, Song Z, Yin G. Energy-optimal routing for electric vehicles using deep reinforcement learning with transformer. Appl Energy 2023;350. https://doi.org/10.1016/j.apenergy.2023.121711.
[5] Gami F, et al. Stochastic optimal reactive power dispatch at varying time of load demand and renewable energsy resources using an efficient modified jellyfish optimizer. Neural Comput Appl 2022;34(22):20395–410. https://doi.org/10.1007/s00521-022-07526-5.
[6] Abaza A, Fawzy A, El-Sehiemy RA, Alghamdi AS, Kamel S. Sensitive reactive power dispatch solution accomplished with renewable energy allocation using an enhanced coyote optimization algorithm. Ain Shams Eng J 2021;12(2):1723–39. https://doi.org/10.1016/j.asej.2020.08.021.
[7] Liu X, et al. Building-centric investigation into electric vehicle behavior: a survey-based simulation method for charging system design. Energy 2023;271. https://doi.org/10.1016/j.energy.2023.127010.
[8] Li X, et al. Electric vehicle behavior modeling and applications in vehicle-grid integration: an overview. Energy 2023;268. https://doi.org/10.1016/j.energy.2023.126647.
[9] Lee G, Song J, Han J, Lim Y, Park S. Study on energy consumption characteristics of passenger electric vehicle according to the regenerative braking stages during real-world driving conditions. Energy Nov. 2023;283:128745. https://doi.org/10.1016/J.ENERGY.2023.128745.
[10] Loni A, Asadi S. Data-driven equitable placement for electric vehicle charging stations: case study San Francisco. Energy 2023;282. https://doi.org/10.1016/j.energy.2023.128796.
[11] Liu Y, Ćetenović D, Li H, Gryazina E, Terzija V. An optimized multi-objective reactive power dispatch strategy based on improved genetic algorithm for wind power integrated systems. Int J Electr Power Energy Syst 2022;136. https://doi.org/10.1016/j.ijepes.2021.107764.
[12] Shaheen MAM, et al. Enhanced transient search optimization algorithm-based optimal reactive power dispatch including electric vehicles. Energy Aug. 2023;277:127711. https://doi.org/10.1016/J.ENERGY.2023.127711.
[13] Yang X, Peng Z, Wang P, Zhuge C. Seasonal variance in electric vehicle charging demand and its impacts on infrastructure deployment: a big data approach. Energy 2023;280. https://doi.org/10.1016/j.energy.2023.128230.
[14] Marcelino CG, Leite GMC, Jimenez-Fernandez S, Salcedo-Sanz S. An improved C-DEEPSO algorithm for optimal active-reactive power dispatch in microgrids with electric vehicles. IEEE Access 2022;10:94298–311. https://doi.org/10.1109/ACCESS.2022.3203728.
[15] Saddique MS, Habib S, Haroon SS, Bhatti AR, Amin S, Ahmed EM. Optimal solution of reactive power dispatch in transmission system to minimize power losses using sine-cosine algorithm. IEEE Access 2022;10:20223–39. https://doi.org/10.1109/ACCESS.2022.3152153.
[16] Karimi S, Hosseini-Hemati S, Rastgou A. Stochastic multi-objective ORPD for active distribution networks. Sustain Energy Technol Assessments 2023;57. https://doi.org/10.1016/j.seta.2023.103235.
[17] Muhammad Y, et al. Fractional memetic computing paradigm for reactive power management involving wind-load chaos and uncertainties. Chaos, Solit Fractals 2022;161. https://doi.org/10.1016/j.chaos.2022.112285.
[18] Chary GVB, Rosalina KM. Analysis of transmission line modeling routines by using offsets measured least squares regression ant lion optimizer in ORPD and ELD problems. Heliyon 2023;9(no. 3). https://doi.org/10.1016/j.heliyon.2023.e13387.
[19] Vilén K, Ahlgren EO. Linear or mixed integer programming in long-term energy systems modeling – a comparative analysis for a local expanding heating system. Energy 2023;283. https://doi.org/10.1016/j.energy.2023.129056.
[20] Gonzalez-Salazar M, Klossek J, Dubucq P, Punde T. Portfolio optimization in district heating: merit order or mixed integer linear programming? Energy 2023;265. https://doi.org/10.1016/j.energy.2022.126277.
[21] Ma K, Zhang R, Yang J, Song D. Collaborative optimization scheduling of integrated energy system considering user dissatisfaction. Energy 2023;274. https://doi.org/10.1016/j.energy.2023.127311.
[22] Shaheen MAM, Hasanien HM, Alkuhayli A. A novel hybrid GWO-PSO optimization technique for optimal reactive power dispatch problem solution. Ain Shams Eng J 2021;12(1):621–30. https://doi.org/10.1016/j.asej.2020.07.011.
[23] Shaheen MAM, Hasanien HM, Al-Durra A. Solving of optimal power flow problem including renewable energy resources using HEAP optimization algorithm. IEEE Access 2021;9:35846–63. https://doi.org/10.1109/ACCESS.2021.3059665.
[24] Ghasemi M, Akbari E, Faraji Davoudkhani I, Rahimnejad A, Asadpoor MB, Gadsden SA. Application of Coulomb's and Franklin's laws algorithm to solve large-scale optimal reactive power dispatch problems. Soft Comput 2022;26(24):13899–923. https://doi.org/10.1007/s00500-022-07417-w.
[25] Qu Z, et al. Dynamic exploitation Gaussian bare-bones bat algorithm for optimal reactive power dispatch to improve the safety and stability of power system. IET Renew Power Gener 2022;16(7):1401–24. https://doi.org/10.1049/rpg2.12428.
[26] Zhao S, Zhang T, Ma S, Wang M. Sea-horse optimizer: a novel nature-inspired meta-heuristic for global optimization problems. Appl Intell 2023;53(10):11833–60. https://doi.org/10.1007/s10489-022-03994-3.
[27] Özbay FA. A modified seahorse optimization algorithm based on chaotic maps for solving global optimization and engineering problems. Eng Sci Technol, Int J 2023;41. https://doi.org/10.1016/j.jestch.2023.101408.
[28] Sharma S, Sabitha B, Prabhakaran A, Chavan M, Srivastava R. A hybrid swarm intelligence approach for resolving reactive power dispatch issues in power system: optimal placement and sizing of UPFC. Adv Eng Software 2022;170. https://doi.org/10.1016/j.advengsoft.2022.103149.
[29] Zhang W, Maleki A. Modeling and optimization of a stand-alone desalination plant powered by solar/wind energies based on back-up systems using a hybrid algorithm. Energy 2022;254. https://doi.org/10.1016/j.energy.2022.124341.
[30] Zhao Y, et al. A new hybrid optimization prediction strategy based on SH-Informer for district heating system. Energy 2023;282. https://doi.org/10.1016/j.energy.2023.129010.

[31] Prasad D, Banerjee A, Singh RP. Optimal reactive power dispatch using modified differential evolution algorithm. Lecture Notes in Networks and Systems, 41; 2019. p. 275–83. https://doi.org/10.1007/978-981-13-3122-0_26/FIGURES/2.

[32] Habib Khan N, Jamal R, Ebeed M, Kamel S, Zeinoddini-Meymand H, Zawbaa HM. Adopting Scenario-Based approach to solve optimal reactive power Dispatch problem with integration of wind and solar energy using improved Marine predator algorithm. Ain Shams Eng J 2022;13(5). https://doi.org/10.1016/j.asej.2022.101726.

[33] Singh B, Bishnoi SK, Sharma M, Singh P, Dhundhara S. An application of nature inspried algorithm based dual-stage frequency control strategy for multi micro-grid system. Ain Shams Eng J 2023;14(9). https://doi.org/10.1016/j.asej.2023.102125.

[34] Sarfraz M, Khan M, Ahmed A. Study of thermophoresis and Brownian motion phenomena in radial stagnation flow over a twisting cylinder. Ain Shams Eng J 2023;14(2). https://doi.org/10.1016/j.asej.2022.101869.

[35] Oyewola OM, Petinrin MO, Labiran MJ, Bello-Ochende T. Thermodynamic optimisation of solar thermal Brayton cycle models and heat exchangers using particle swarm algorithm. Ain Shams Eng J 2023;14(4). https://doi.org/10.1016/j.asej.2022.101951.

[36] MATPOWER – Free, open-source tools for electric power system simulation and optimization." Accessed: January. 15, 2023. [Online]. Available: https://matpower.org/.

[37] Alternative Fuels Data Center: Electric Vehicle Infrastructure Projection Tool (EVI-Pro) Lite. Accessed: August. 08, 2023. [Online]. Available: https://afdc.energy.gov/evi-pro-lite?utf8=%E2%9C%93&load_profile%5Bstate%5D=MO&load_profile%5Burban_area%5D=St.+Louis&load_profile%5Bstate_name%5D=Missouri&load_profile%5Bfleet_size%5D=1000&load_profile%5Bmean_dvmt%5D=35&load_profile%5Bclass_dist%5D=Sedan&load_profile%5Bwork_power_dist%5D=MostL2&load_profile%5Bhome_access_dist%5D=HA100&load_profile%5Bhome_power_dist%5D=Equal&load_profile%5Bpref_dist%5D=Home100&commit=Calculate.

[38] Hasanien HM, Alsaleh I, Alassaf A, Alateeq A. Enhanced coati optimization algorithm-based optimal power flow including renewable energy uncertainties and electric vehicles. Energy 2023;283. https://doi.org/10.1016/j.energy.2023.129069.